

Research Article

Optimal BESS Sizing for Industrial Facilities Participating in RTP DR

Youssef Shakrina , Rayan Al Sabbahi , and Harag Margossian 

Lebanese American University, Beirut, Lebanon

Correspondence should be addressed to Harag Margossian; harag.margossian@gmail.com

Received 20 April 2023; Revised 5 September 2023; Accepted 12 September 2023; Published 6 October 2023

Academic Editor: Qiuye Sun

Copyright © 2023 Youssef Shakrina et al. This is an open access article distributed under the Creative Commons Attribution License, which permits unrestricted use, distribution, and reproduction in any medium, provided the original work is properly cited.

The predictability of their manufacturing lines allows industrial facilities to optimize their production scheduling and to participate in demand response (DR), in day-ahead, real-time pricing (RTP) electricity markets. Battery energy storage systems (BESSs) make the electrical demand of industrial facilities more flexible and increase their potential to benefit from DR. The BESS sizing problem, for industrial facilities participating in RTP DR, is complex due to the discreteness of their manufacturing lines and the stochastic nature of electricity pricing. In this paper, an approach to BESS sizing is proposed. Scenario extraction using *k*-means clustering is used to reduce the problem complexity, and the extracted scenarios are preprocessed to reduce the search space for the optimal size of the BESS. The steps involved in the proposed approach are demonstrated, in detail, through a case study that uses a generic model of an industrial unit. The results of the case study show the effectiveness and validity of the problem reduction techniques used and highlight the role of electricity storage in maximizing the profits of the industrial unit. Finally, a sensitivity analysis is carried out to illustrate the impact of the BESS installation cost on the results.

1. Introduction

Real-time pricing (RTP) in day-ahead electricity markets is used to induce a change in the load patterns of consumers as part of a mechanism known as demand response (DR) [1, 2]. For the operator, DR is an ancillary service used to support the operation of the grid [3–5] while reducing costs [6, 7] and emissions [8]. Meanwhile, consumers, by being aware of electricity prices, benefit from DR by optimizing their consumption patterns and minimizing their costs.

Modeling of DR from the perspective of the consumer depends on the type of the consumer considered. Residential consumers are often highly responsive with sheddable, nonsheddable, and shiftable loads [9]. In [10], the authors divide home appliances into categories based on their energy consumption and operation characteristics. They then propose a load scheduling algorithm that maximizes consumer value while considering budget constraints. A home energy management system that minimizes cost while penalizing discomfort generated by load shifts is proposed in

[11]. Community-based modeling of residential DR is studied in [12, 13].

Commercial consumers are the least responsive due to fixed activity hours [9]. However, heating and cooling systems can be controlled to adjust electricity consumption patterns while not affecting the level of thermal comfort of the people in the building, as shown in [14, 15].

Industrial loads are the most elaborate to model. They have a certain level of predictability due to the use of manufacturing lines; this allows for more accurate demand optimization used to minimize energy consumption or maximize profit. Specialized models for the meat, cement, and food industries are presented in [16, 17], and [18], respectively. These models support manual decision-making in response to RTP or offered incentives. An automated response to the real time, incentive-based DR programs of discrete manufacturing facilities is proposed in [19]. The authors formulate the profit maximization problem to automatically determine optimal electrical load reduction and product manufacturing strategies. In [20], the authors

propose a new model for the demand for aluminum, steel, and cement factories as part of a single microgrid. They formulate the profit maximization problem with a focus on the cooperation among the factories and the interaction with the microgrid. A data-driven model of RTP DR is proposed in [21]. The authors use long short-term memory recurrent neural networks (LSTM RNNs) to account for uncertainty in future electricity prices and determine an optimal energy management strategy.

These prior studies show that industrial consumers have a lot to gain by participating in DR. Nevertheless, the level of optimization possible is restricted by the limited flexibility of their manufacturing lines. In addition, due to their discrete manufacturing processes, industrial loads can only change their demand in discrete kW or MW values, making their DR more rigid [22, 23]. These limitations in flexibility and granularity can be circumvented using battery energy storage systems (BESSs).

In the open literature, research on BESS has been focused on its role as a provider of ancillary services in active distribution grids, microgrids, and hybrid standalone supply systems. Essential services that the BESS can provide include voltage regulation [24], frequency control [25], and energy balancing [26]. In the context of industrial facilities, the role of BESS is to help reduce the electricity bill or to increase the profits of these facilities. This can be achieved by charging the BESS during periods with low electricity prices and either using the charged energy during periods where prices are high or selling the energy back to the grid for additional profit.

Energy management of industrial facilities with discrete manufacturing models and energy storage is studied in [27–29]. In [27], the authors formulate an optimal load dispatch problem of industrial consumers, with distributed energy resources (DERs) and energy storage, in response to RTP. Their objective is to minimize the cost of these consumers, including fuel, DER maintenance, and electricity purchasing cost, while meeting a given target for product manufacturing. In [28], a model that determines the load reduction capability of industrial consumers in response to incentive-based DR is presented. The model minimizes the completion time of the manufacturing process for a given set of product orders while reducing electricity purchasing costs and considering electricity storage and PV production. The authors in [29] present a scenario-based stochastic model to minimize the electricity cost and the battery operation cost for an industrial unit equipped with a PV production source. The authors provide a detailed discrete assembly line model and an elaborate BESS model for healthier battery utilization. The optimization problem is then solved with a hybrid method considering differential evolution techniques and branch and bound-based solvers. In these papers, the authors considered a fixed or a minimum manufacturing output and a predetermined BESS capacity.

Optimal sizing of BESS is often studied in conjunction with their optimal placement. Their ability to provide ancillary services plays an important role in this regard. BESS sizing for industrial facilities, on the other hand, is more dependent on the structure of these facilities. There are several articles that have proposed approaches to size the

BESS for industrial consumers. In [30], the authors provided a bilevel stochastic optimization model to determine the capacity of the energy storage unit. The objective of the BESS is to maximize the annual expected net benefit from the economic impact energy storage has on the electricity bill. The model considers a k -means clustering algorithm to generate a typical load profile for the industrial unit. In [31], genetic algorithm is utilized to optimally size the BESS for industrial prosumers to attain high energy savings with fast payback periods. The authors verify their model under four energy management strategies for an industrial load profile and a solar production profile over a year. To minimize the electricity bill for industrial consumers with BESS, the authors in [32] provided an approach considering decision theory. The paper considers probabilistic techniques and uncertainties to optimally size the energy storage given a load profile. While all the previous approaches considered a typical industrial unit load profile, the authors in [33] generated this demand from an integrated simulation model for manufacturing load. This load is thereafter used to optimally size the BESS in addition to other renewable generation sources to minimize the yearly electricity billing cost using linearization and meta-heuristic strategies.

To make full use of the BESS, an industrial facility's energy management should maximize its profit rather than only satisfy a manufacturing duty. In addition, it should consider its elaborate manufacturing scheme and account for diverse electricity pricing scenarios. This merge of discrete manufacturing lines with multiple scenarios increases the computational complexity and makes the problem difficult to be solved.

The main contributions of the paper are as follows:

- (1) The approach proposed in this paper considers a comprehensive model of industrial facilities with discrete manufacturing processes. The models proposed in [30–32] do not consider the discrete nature of the manufacturing processes, while in [33], the authors only extract the load profile from the complete manufacturing model but do not include the model itself in the optimization.
- (2) To overcome the computational challenges of solving the model, problem reduction techniques are proposed:
 - (a) A method is introduced to extract representative scenarios for electricity pricing from a historical dataset
 - (b) The search space is limited by precomputing, upper and lower bounds for BESS capacity
- (3) The proposed model is used to illustrate the role that electricity storage can play in maximizing the profits of the industrial facilities.

The remainder of this paper is divided as follows: Section 2 models the industrial facility operation and the energy storage management and sizing. Section 3 proposes the scenario reduction and solving techniques. Section 4 provides a case study to demonstrate the sizing model and analyze the impact of BESS. Finally, Section 5 concludes the paper.

2. BESS Sizing Optimization

In this section, the stochastic optimization problem of the BESS sizing of a complex industrial facility is presented. The model includes an industrial facility that aims to maximize its manufacturing output while minimizing its costs, including purchasing the items, electrical power needed for manufacturing, and labor. With the addition of the BESS, the facility can (1) optimally schedule the operation of each manufacturing unit, (2) purchase the items necessary for production, and (3) manage the charging and discharging of the BESS. The mathematical model of each of the components is provided in the following subsections.

2.1. Manufacturing Model of the Industrial Facility. The model used for the discrete manufacturing process of an industrial facility in this paper is based on that presented in [19]. This process is represented in the form of manufacturing lines and an assembly line that collects the created items to produce a final product. A schematic example of the model is shown in Figure 1.

The assembly line is assigned row 0, and the manufacturing lines are assigned rows 1 to R .

Each machine produces items that are fed to a buffer to be stored. The items in those buffers are then used by the following machine in the line. The machines and buffers are numbered according to their location in the different lines.

Machines are represented by squares, and buffers are represented by circles.

The machines and buffers are modeled as follows:

$$B_{ijt} = B_{ij(t-1)} + n_{ijt} - \alpha_{ij} n_{i(j+1)t}, t \in T; i = 0, \dots, R; j = 1, \dots, M_i - 1, \quad (2)$$

where α_{ij} is the number of parts needed for a machine at row i , column j to provide for the next machine to produce a single item.

- (2) Buffers at the end of nonassembly lines ($i \neq 0$) feeding the first machine at the assembly line ($i=0$). Their storage level at time t is defined by

$$B_{ijt} = B_{ij(t-1)} + n_{ijt} - \alpha_{ij} n_{01t}, t \in T; i = 1, \dots, R; j = M_i. \quad (3)$$

- (3) The buffer at the end of the assembly line accumulates all the produced goods. This buffer does not feed any other machine and its storage level at time t is given by

$$B_{ijt} = B_{ij(t-1)} + n_{ijt}, t \in T; i = 0; j = M_0. \quad (4)$$

Moreover, the buffers have capacity limits modeled by

$$0 \leq B_{ijt} \leq \overline{B}_{ij}, t \in T; i = 0, \dots, R; j = 1, \dots, M_i. \quad (5)$$

The number of items stored in the last buffer of the assembly line in period t_{24} represents the final number of produced items in the day and is defined as follows:

Machines: the role of a machine is to manufacture items in a certain period t .

The operational status of a machine can be categorized as either active or inactive. There are several reasons for a machine to be inactive, ranging from high electricity prices to situations, where the manufacturing line is unable to accommodate more machines due to a full buffer.

x_{ijt} is a binary variable that is used to identify whether, in period t , the machine at row i and column j is on ($x_{ijt} = 1$) or off ($x_{ijt} = 0$).

The number of items produced by the machine (n_{ijt}) is given by the following equation:

$$n_{ijt} = \frac{T_s}{CT_{ij}} x_{ijt}, t \in T; i = 0, \dots, R; j = 1, \dots, M_i, \quad (1)$$

where T_s is the length of the time slot in s and CT_{ij} is the cycling time of the machine at row i and column j , in s .

Buffers: the role of a buffer is to store manufactured items that will be used later. Generally, the number of items in a buffer in period t is the number of items in period $t - 1$ plus the number of items manufactured by the machine preceding it and minus the number of items used by the machine following it. In [18], three types of buffers are defined, depending on their location:

- (1) Buffers in all rows and columns, except the ones at the end of each line, feed the machine following it. The number of items in the buffer in period t , B_{ijt} , is expressed as given in the following equation:

$$f = B_{0M_0t_{24}}. \quad (6)$$

The following additional constraints define the operation of the manufacturing process:

- (1) A machine is off in period t ($x_{ijt} = 0$) if the buffer before it was empty in the previous period. This applies to all machines except the first one of the assembly line. The inequality expressed in equation (7) satisfies this condition:

$$x_{i(j+1)t} \leq B_{ij(t-1)}, t \in T; i = 0, \dots, R; j = 1, \dots, M_i - 1. \quad (7)$$

- (2) The first machine in the assembly line needs the last buffers in all manufacturing lines to not be empty for it to operate. This is achieved by

$$x_{01t} \leq B_{ij(t-1)}, t \in T; i = 1, \dots, R; j = M_i. \quad (8)$$

- (3) A machine in period t cannot operate if the buffer following it was full in period $t - 1$; equation (9) ensures this constraint:

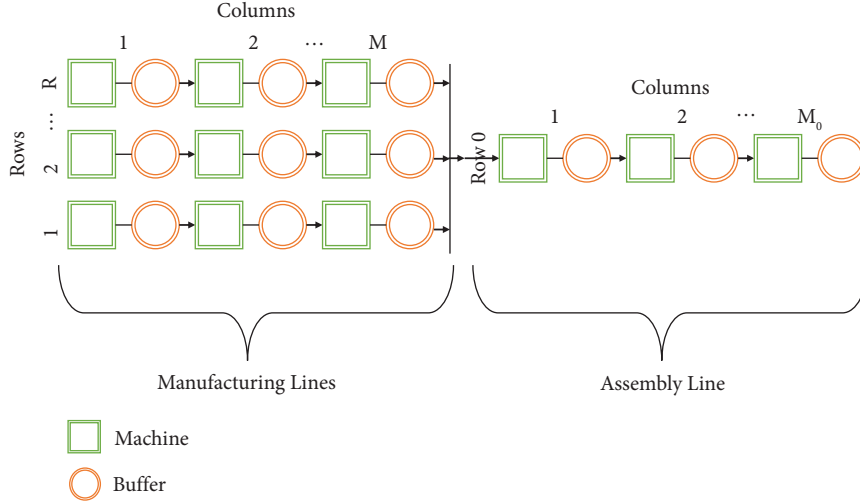


FIGURE 1: Industrial manufacturing process.

$$x_{ijt} \leq B_{ij} - B_{ij(t-1)}, t \in T; i = 0, \dots, R; j = 1, \dots, M_i. \quad (9)$$

2.2. *The BESS Model.* The state of charge of the BESS in a period t , SoC_t , equals the state of charge in the previous period plus the energy charged in period t , Ec_t , minus the energy discharged in period t , Ed_t :

$$\text{SoC}_t = \text{SoC}_{t-1} + \text{Ec}_t - \text{Ed}_t, t \in T. \quad (10)$$

The BESS is assumed to have a given initial state of charge at the start of the day and a given final state of charge at the end of the day, defined as a certain percentage, π , of its capacity, SoC . Therefore, as a special case of equation (10), the state of charge in periods t_1 and t_{24} are given as follows:

$$\text{SoC}_{t_1} = \pi \cdot \overline{\text{SoC}} + \text{Ec}_t - \text{Ed}_t, \quad (11)$$

$$\text{SoC}_{t_{24}} = \text{SoC}_{t_{24-1}} + \text{Ec}_t - \text{Ed}_t = \pi \cdot \overline{\text{SoC}}. \quad (12)$$

The BESS has an upper storage capacity limit

$$0 \leq \text{SoC}_t \leq \overline{\text{SoC}}, t \in T. \quad (13)$$

The BESS cannot instantly charge or discharge. These limits are shown in equations (14) and (15). In addition, the BESS is assumed not to be able to charge and discharge at the same time, determined by the variable x_{c_t} .

$$0 \leq \text{Ec}_t \leq \overline{\text{Ec}} \cdot x_{c_t}, t \in T, \quad (14)$$

$$0 \leq \text{Ed}_t \leq \overline{\text{Ed}} \cdot (1 - x_{c_t}), t \in T. \quad (15)$$

2.3. *Connection to the Supply Grid.* The industrial facility is connected to the electrical supply grid and is capable of buying and selling electricity to the grid. The amount of energy to be exchanged with the supply grid, D_t , is defined by equation (16), and includes

- (i) The energy consumed by each of the machines during operation.
- (ii) A small amount of energy that is consumed by the machines even when they are off [19].
- (iii) The energy exchanged with the BESS. This includes a charging efficiency, η_C , is to reflect the energy losses while charging the BESS and a discharging efficiency, η_D , used to reflect the energy losses while discharging the BESS.

$$D_t = \sum_{i=0}^R \sum_{j=1}^{M_i} (x_{ijt} \cdot \text{Pon}_{ij} + (1 - x_{ijt}) \cdot \text{Poff}_{ij}) \cdot \frac{\text{Ts}}{3600} + \frac{\text{Ec}_t}{\eta_C} - \text{Ed}_t \cdot \eta_D, t \in T. \quad (16)$$

The amount of energy that can be exchanged with the supply grid is limited based on the electrical point of connection. This is satisfied with the following equation:

$$-LL \leq D_t \leq LL, t \in T. \quad (17)$$

2.4. *The Optimization Model.* The goal of the industrial facility is to maximize its profit that is defined by the following terms:

- (1) The revenue from selling the final products is given by

$$\text{revenue} = f \cdot v, \quad (18)$$

where f is the final number of produced goods and v is the price per good, in cents.

- (2) The labor cost of manufacturing is given by

$$\text{labor cost} = f \cdot l, \quad (19)$$

where l is the labor cost in cents per product produced.

- (3) The cost of purchasing the items required for the manufacturing process is given by

$$\text{purchased items cost} = \sum_{t=1}^T \sum_{i=1}^R K_{p_{i1}} \cdot \beta_{i1} \cdot n_{i1t}, \quad (20)$$

where β_{i1} is the number of items purchased to operate the machine in row i , column 1, and $K_{p_{i1}}$ is the price of each of these items.

- (4) The cost of electricity consumption is given by

$$\text{electricity cost} = \sum_{t=1}^T D_t \cdot P_t, \quad (21)$$

where P_t is the day-ahead electricity market price in cents/kWh in period t .

- (5) The investment cost of the BESS is given by

$$\text{BESS cost} = \kappa \cdot \overline{\text{SoC}}, \quad (22)$$

where $\overline{\text{SoC}}$ is the capacity of the installed BESS and κ is the equivalent investment cost in cents, per day, per kWh.

The objective function of maximizing profit is finally given as follows:

$$\begin{aligned} \max \text{OF} = & f \cdot v - f \cdot l - \sum_{t=1}^T \sum_{i=1}^R (K_{p_{i1}} \cdot \beta_{i1} \cdot n_{i1t}) \\ & - \sum_{t=1}^T D_t \cdot P_t - \kappa \cdot \overline{\text{SoC}}. \end{aligned} \quad (23)$$

However, due to the stochastic nature of the day-ahead prices, the decision variables and outcomes of the objective function cannot be deterministic and should be taken to be their expected values instead. The objective function is, therefore, modified as follows:

$$\max \text{OF} = \mathbb{E} \left(\tilde{f} \cdot v - \tilde{f} \cdot l - \sum_{t=1}^T \sum_{i=1}^R (K_{p_{i1}} \cdot \beta_{i1} \cdot \tilde{n}_{i1t}) - \sum_{t=1}^T \tilde{D}_t \cdot \tilde{P}_t \right) - \kappa \cdot \overline{\text{SoC}}. \quad (24)$$

In [34], the authors transformed the stochastic variables into a probability density function (PDF). In the proposed model, daily ds scenarios are considered each with a probability γ^{ds} .

The PDF of these scenarios is thus obtained, and equation (24) is rewritten as follows:

$$\max \text{OF} = \sum_{ds=1}^{DS} \gamma^{ds} \cdot \left(f^{ds} \cdot v - f^{ds} \cdot l - \sum_{t=1}^T \sum_{i=1}^R (K_{p_{i1}} \cdot \beta_{i1} \cdot n_{i1t}^{ds}) - \sum_{t=1}^T (D_t^{ds} \cdot P_t^{ds}) \right) - \kappa \cdot \overline{\text{SoC}}. \quad (25)$$

For every period t , the total probability of the market prices must add to one:

$$\sum_{ds=1}^{DS} \gamma^{ds} = 1, t \in T. \quad (26)$$

With the nature of the variables and the constraints used, the BESS sizing optimization problem is now formulated as a mixed integer nonlinear programming (MINLP) model. Note that MINLP problems have increased complexity compared to MILP or NLP problems and require advanced solution methods [35]. All of the MINLP optimization problems presented in this paper were implemented and solved in GAMS.

3. Optimization Problem Reduction

Solving the stochastic problem presented in equation (25), while considering many scenarios, imposes a high computational burden. This is due to the use of integer variables to define the discrete manufacturing processes of the industrial facility and the energy management of the BESS. In

fact, if too many scenarios are considered, the problem becomes nearly impossible to solve even with state-of-the-art solvers and powerful computer hardware. To circumvent these issues, in this section, problem reduction techniques are proposed.

3.1. Scenario Extraction from Historical Data. It is not possible to consider all variation scenarios of the electricity price for a given set of historical data (data over a year or over multiple years). Thus, it is important to identify selected scenarios that well represent the data. To this end, k -means clustering is proposed.

k -means is an unsupervised machine learning algorithm that partitions a dataset into distinct, nonoverlapping groups called clusters, where each data point belongs to only one group [36, 37]. The algorithm aims to make the intracluster data points as similar as possible while also keeping clusters as far as possible from each other. The fewer variations inside a cluster, the more homogenous and similar are its data points. k -means is very fast and is a standard method with many available implementations [38]. It is used to reduce the

number of days in the historical dataset into K representative scenarios.

More formally, k -means adopts an expectation-maximization approach to solve a clustering problem as seen in Algorithm 1 [38].

Each day from the historical data DS is represented by a vector $V_{ds} = \langle P_{t0}, \dots, P_{t23} \rangle$ consisting of the day-ahead market prices that will be partitioned into clusters. Each vector is assigned to a cluster c based on sharing the minimum Euclidean distance to its centroid C_c compared to other centroids, where the distance is computed as follows:

$$d(V_{ds}, C_c) = \sqrt{\sum_{t=0}^{T-1} (P_t - c_t)^2}, \quad (27)$$

where c_t designates centroid price in a period t . The representative scenario in each cluster is the day that has day-ahead market prices with the smallest distance to the cluster's mean.

3.2. Search Space Limitation. Even with the limited number of representative scenarios, it is difficult to solve the proposed stochastic optimization problem. To further reduce the problem complexity, it is proposed to limit the search space for $\overline{\text{SoC}}$, the BESS capacity variable. This is done by preprocessing each of the individual scenarios using the discrete objective function in equation (23) and identifying the minimum and maximum optimal values of SoC. These are then used as upper and lower limits on the BESS capacity, while solving the stochastic problem.

3.3. Approach Summary. The presented approach is illustrated in Figure 2 and summarized as follows:

- (1) Reduce the number of scenarios DS in the historical dataset into K scenarios by using k -means clustering algorithms
- (2) Choose a representative scenario from each cluster
- (3) Find the optimal energy storage $\overline{\text{SoC}}$ for each of the scenarios separately considering the objective function in equation (23)
- (4) Identify the maximum and the minimum optimal values of $\overline{\text{SoC}}$ from the individual scenarios, and use these as upper and lower limits on the BESS capacity
- (5) Solve for the objective function presented in (25) with the K scenarios and the new capacity constraint

4. Case Study

In this section, a motivating example that demonstrates the proposed approach is presented.

4.1. System Description. The schematic diagram of the industrial facility is shown in Figure 3. The characteristics and the parameters of the machines are listed in Table 1.

The selling price of the product is $v = \text{€}9.30$. The labor cost of each product is $l = \text{€}1.20$. All the machines are assumed to consume $\text{Poff}_{ij} = 1 \text{ kW}$ when turned off. The day studied is divided into 24 hours ($T_s = 3600 \text{ s}$). Historical data of day-ahead hourly prices (P_t) of Finland from the years 2019 and 2020 are considered [39].

The charging and discharging limits of the BESS are set to 30% of its maximum capacity, such that $\overline{E_c} = \overline{E_d} = 0.3 \cdot \overline{\text{SoC}}$. The charging and discharging efficiencies are taken to be: $\eta_c = 95\%$ and $\eta_D = 80\%$, respectively. The BESS is assumed to be 40% full at the beginning and the end of each day ($\pi = 0.4$). Finally, the line connected to the industrial load has a thermal limitation of $\text{LL} = 600 \text{ kW}$.

4.2. Scenario Extraction. The first step to finding the optimal BESS size that would maximize the profit of the industrial facility presented in Section 4.1 is to extract representative scenarios from the historical data. The day-ahead price data of Finland from the years 2019 and 2020 includes 731 different scenarios, i.e., $\text{DS} = 731$. The objective of the scenario extraction is to reduce the number of scenarios to K scenarios; for this study, K is chosen to be 12.

Using k -means clustering, the 731 scenarios are therefore partitioned into 12 clusters. The different dips and peaks of the prices in terms of occurrences and magnitude signify the alterations and the diversity in the market prices extracted by the k -means algorithm. After the clusters are formed, a representative scenario for each of the clusters is chosen based on (27).

Figures 4 and 5 show all the grouped scenarios in two of the clusters, k_{10} and k_{12} , as well as the representative scenario for these clusters. Despite having some outliers, the obtained clusters show price variations that are consistent with each other in terms of shape and magnitude. This highlights the effectiveness of k -means in grouping similar day-ahead market prices together.

The representative scenarios of all 12 clusters are displayed in Figure 6.

To get the PDF of the selected scenarios, the probability γ_k of the representative scenarios is obtained by dividing the number of scenarios in the cluster by the total number of scenarios DS in the dataset. The results are shown in Table 2.

4.3. Preprocessing Scenarios. Once the representative scenarios are identified and their probabilities are determined, the scenarios are preprocessed to find upper and lower bounds for the BESS capacity variable $\overline{\text{SoC}}$. This results in a reduced search space for the stochastic BESS sizing problem. To this end, 12 optimization problems are solved, maximizing (23), while subject to equations (1)–(17).

The results are shown in Table 3.

Based on these results, additional variable limits on the BESS capacity are introduced, given by

$$0 \leq \overline{\text{SoC}} \leq 6562. \quad (28)$$

- (1) Specify the number of k clusters to assign.
- (2) Randomly initialize k centroids.
- (3) **repeat**
- (4) **expectation**: Assign each point to its closest centroid.
- (5) **maximization**: Compute the new centroid (mean) of each cluster.
- (6) **until** The centroid positions do not change.

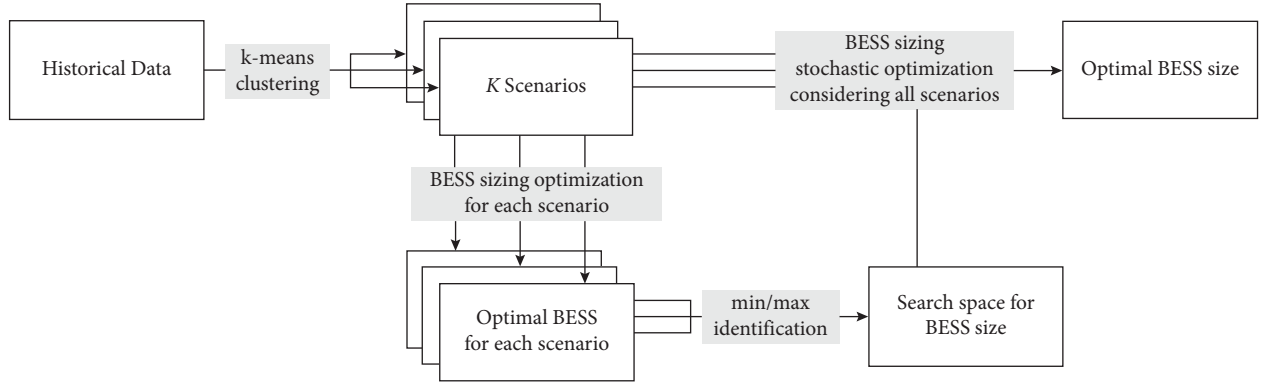
ALGORITHM 1: k -means algorithm.

FIGURE 2: Proposed approach for optimization problem reduction.

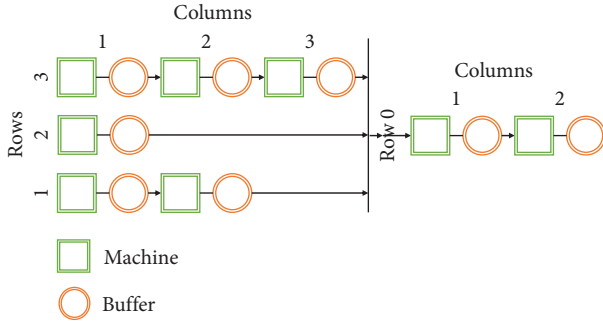
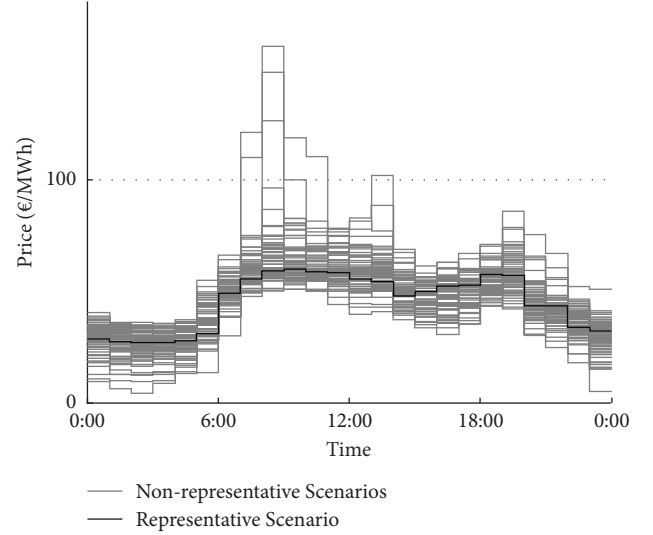


FIGURE 3: Schematic diagram of studied industrial load.

TABLE 1: Industrial facility parameters.

	CT_{ij} (s)	\bar{B}_{ij}	Pon_{ij} (kW)	α_{ij}	K_{il} (cents)	β_{il}	
Machine	$i1.j1$	50	350	65	3	20	3
	$i1.j2$	300	55	43	1	—	—
	$i1.j3$	300	55	31	2	—	—
	$i2.j1$	50	350	65	3	20	3
	$i3.j1$	60	120	81	2	20	3
	$i3.j2$	90	80	65	1	—	—
	$i0.j1$	300	50	65	1	—	—
	$i0.j2$	360	2000	74	—	—	—

4.4. Final Results and Analysis. After finding the upper and lower bounds for the BESS capacity, the optimization problem with the objective function presented in (25) and subject to equations (1)–(17). This results in an optimal storage capacity of 5624 kWh.

FIGURE 4: Grouped scenarios in $k10$.

4.4.1. Result Verification. To assess these results, the energy management optimization problem, with the objective function in (23), is assessed with a fixed BESS size of 5624 kWh for all original 731 scenarios. The real average profit (RAP) over the studied dataset is then calculated as follows:

$$RAP = \sum_{ds=1}^{DS} \frac{OF^{ds}}{DS}, \quad (29)$$

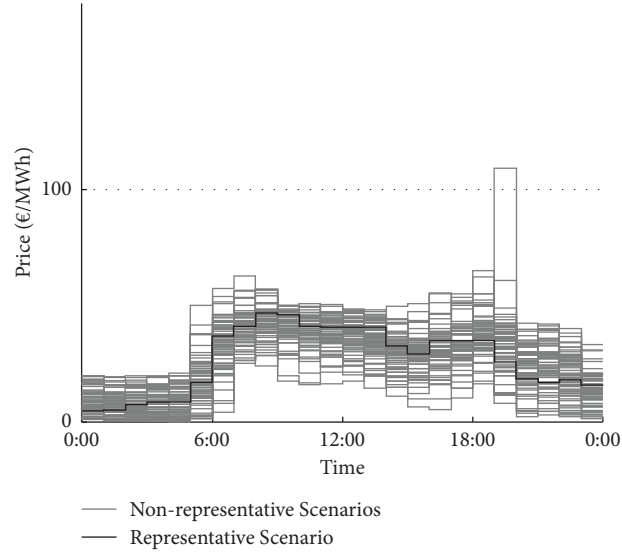
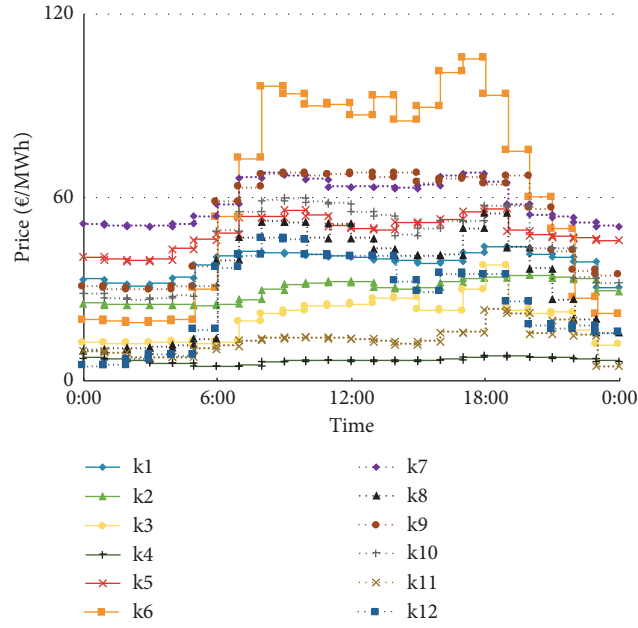
FIGURE 5: Grouped scenarios in k_{12} .

FIGURE 6: Representative scenarios of the 12 clusters.

TABLE 2: Probability of each scenario.

Scenario k	1	2	3	4	5	6	7	8	9	10	11	12
γ^k	0.1423	0.0807	0.0999	0.0534	0.1094	0.0150	0.0465	0.1012	0.0930	0.0917	0.0711	0.0958

TABLE 3: Optimal BESS capacity of each scenario.

Scenario k	1	2	3	4	5	6	7	8	9	10	11	12
$\overline{\text{SoC}}$ (kWh)	1644	0	3565	0	0	6561	0	3152	5624	5624	3278	4325

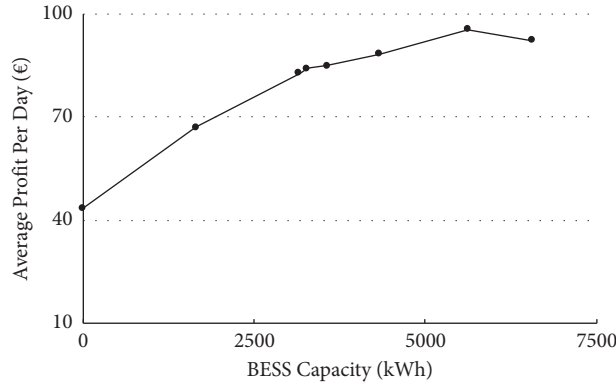


FIGURE 7: Average profit per day for different BESS capacities.

where OF^{ds} is the objective function value of scenario ds .

This yielded a real average daily profit of €95.54.

This task was then repeated for the different values of \overline{SoC} obtained from each of the 12 extracted scenarios. The daily profit vs. different storage capacities is shown in Figure 7. Over the course of the studied period, the average daily profit for the industrial unit without installing BESS is €43.44, less than half of the profit attained by the optimal BESS capacity of 5624 kWh. On the other hand, using the highest optimal capacity obtained from scenario $k6$ (6561 kWh), the average daily profit is €92.29, 3.4% less compared to the optimal capacity.

4.4.2. Impact of considering Several Scenarios. To illustrate the importance of the proposed approach of extracting multiple scenarios, a direct comparison is made with the results of taking the two studied years as a single scenario, i.e., having a single average representative for each hour in the 24-hour study period. The average of the scenarios, calculated based on (27), is shown in Figure 8.

With $DS = 731$ days and $\kappa = 0.1$ cents/kWh, the optimization model yielded an optimal storage size of $\overline{SoC} = 2843.667$ kWh.

The real average profit of all days in the dataset, computed using (29), is €82.24, resulting in a decrease of 13.92%, compared to the optimal BESS size of 5624 kWh.

4.4.3. Sensitivity Analysis. Sensitivity analysis is carried out for different values of κ to study the impact of installation costs on the sizing. The simulation results are illustrated in Table 4.

The case study results illustrate the significance of energy storage and the importance of low BESS costs in increasing profit.

At low installation costs $\kappa = 0.01$ cents/kWh, the average daily profit was €97.24 with a high optimal storage capacity of 6561 kWh.

With higher installation prices $\kappa = 0.5$ cents/kWh, a lower optimal energy storage capacity is needed (2974 kWh), and lower profit becomes attainable (€85.86). If the installation prices become high enough, the BESS will no longer make economic sense, and therefore the

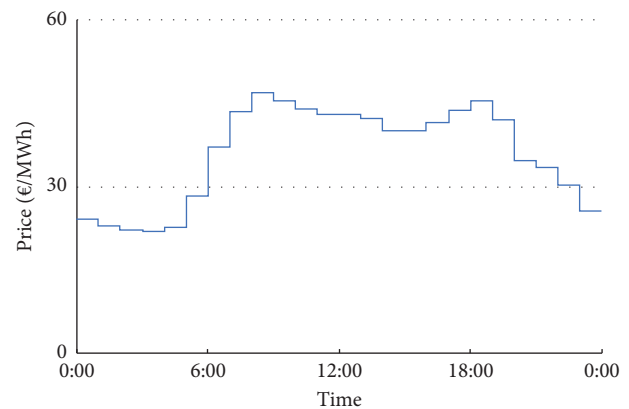


FIGURE 8: Representative average scenarios.

TABLE 4: Profit and optimal storage capacity for different BESS installation prices.

κ (cents/kWh)	\overline{SoC} (kWh)	RAP (€)
0.01	6561	97.24
0.1	5624	95.54
0.5	2974	85.86
1	1890	57.62
3	0	43.44

industrial facility is better off without it, as in the case when $\kappa = 3$ cents/kWh. The average profit in this case would be €43.44.

For a more comprehensive analysis of the impact of installation costs and BESS capacities, the previous sensitivity analysis was expanded to also include the different BESS capacities considered in Section 4.4.1. The results are shown in Figure 9.

As expected, the highest average daily profit is observed at the values indicated in Table 4. For instance, when the installation cost is 0.01 cents/kWh, the industrial unit achieves maximum profitability with a battery size of 6561 kWh. Conversely, when the installation cost is high, at 3 cents/kWh, the industrial unit generates less profit compared to the €43.44 it gets without any battery installed.

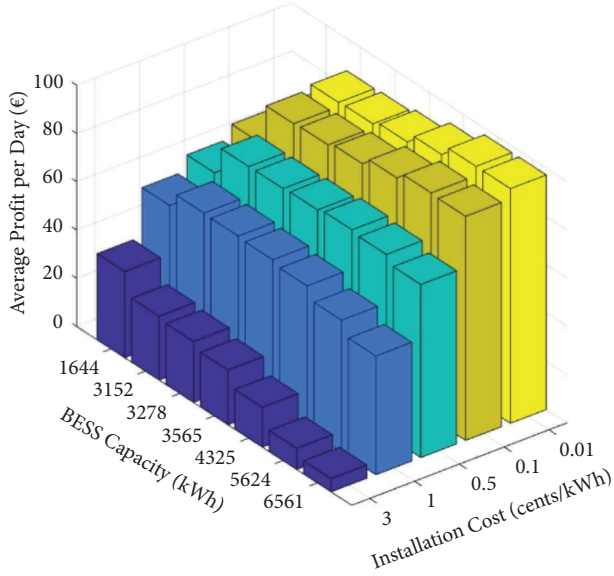


FIGURE 9: Average profit per day for different BESS capacities for different installation costs.

5. Conclusion

In this paper, the response of industrial demand to real-time pricing was considered, with a focus on the impact of energy storage. A BESS sizing approach, based on a profit-maximizing model for the energy management system, was presented. The model considers the discrete manufacturing processes of industrial facilities and relies on stochastic modeling of energy prices based on historical data. Scenario reduction using k-means clustering and preprocessing the data to limit the search space were proposed to mitigate problem complexity. A detailed case study based on a generic industrial consumer was presented. The effectiveness of the approach was verified by comparing the expected profit to the simulated profit over the studied period. Moreover, a sensitivity analysis was carried out to show the impact of the cost of installation of energy storage on its feasibility. Future work will be focused on extending the model to consider different types of demand response programs, including time-of-use pricing, demand-side bidding, and incentive-based programs.

Nomenclature

List of Acronyms

BESS: Battery energy storage system
 DER: Distributed energy resources
 DR: Demand response
 MINLP: Mixed integer nonlinear programming model
 PDF: Probability density function
 RTP: Real-time pricing

Sets

DS: Set of all day-ahead market prices scenarios
 K: Set of representative day-ahead market prices scenarios
 M_R: Set of machines in every element of set R

R: Set of serial production line branch

T: Set of time periods

Real Variables

B_{ijt} : Quantity of items stored in a buffer at row i , column j in period t
 D_t : Energy bought by the industrial facility from the grid in kWh
 \widetilde{D}_t : Expected energy bought by the industrial facility from the grid in kWh
 D_t^{ds}/D_t^k : Energy bought by the industrial facility from the grid in kWh in a scenario ds/k
 Ec_t : Energy charged in the BESS in a period t in kWh
 Ed_t : Energy discharged from the BESS in a period t in kWh
 f_t : Number of final products produced
 \widetilde{f}_t : Expected number of final products produced
 f_t^{ds}/f_t^k : Number of final products produced in a scenario ds/k
 n_{ijt} : Quantity of items that a machine at row i , column j generates in a period t
 \widetilde{n}_{ijt} : Expected quantity of items that a machine at row i , column j generates in a period t
 n_{ijt}^{ds}/n_{ijt}^k : Stochastic quantity of items that a machine at row i , column j generates in a period t in a scenario ds/k
 SoC_i : BESS's state of charge in kWh
 \widetilde{SoC} : BESS's capacity in kWh

Binary Variables

xc_t : On/off indicator of the BESS charging status
 x_{ijt} : On/off indicator of a machine at row i , column j in period t

Parameters

\overline{B}_{ij} : Maximum storage capacity of buffer at row i , column j
 C_c : Centroid of the cluster
 C_t : Centroid price in a period t
 CT_{ij} : Cycling time of a machine at row i , column j in s
 d : Euclidean distance between the vector of day-ahead market prices and the cluster's centroid
 \overline{Ec} : Maximum energy charged in period t in kWh
 \overline{Ed} : Maximum energy discharged in period t in kWh
 Kp_{i1} : Price of every β_{i1} in cents
 l : Labor cost per product produced in cents
 LL: Line limit in kW
 $Poff_{ijt}$: Power demand of a machine at row i , column j in a period t when turned off in kW
 Pon_{ijt} : Power demand of a machine at row i , column j in a time slot when turned on in kW
 P_t : Day-ahead market price in cents/kWh in a period t
 \widetilde{P}_t : Expected day-ahead market price in cents/kWh in a period t
 P_t^{ds}/P_t^k : Market price of a scenario ds/k in a period t in cents/kWh
 RAP: Real average profit per day in the studied period
 Ts: Length of the time slot in s

- v : Market price per product produced in cents
 V_{ds} : Vector containing the day-ahead market price of each day in the dataset
 α_{ij} : Number of parts needed for a machine at row i , column j to provide for the next machine to produce one item
 β_{i1} : Number of items purchased to operate the machines in the first columns
 γ^{ds}/γ^k : Probability of a market price in scenario ds/k
 η_C : Charging efficiency
 η_D : Discharging efficiency
 κ : BESS's equivalent installation costs per day in cents/kWh
 π : Percentage of charge the BESS has at the beginning and the end of the day

Objective Functions

- OF: Profit of industrial facility without BESS installation costs
 OF2: Expected profit of industrial facility with BESS installation costs
 OF2^{ds}: Profit of industrial facility with BESS installation costs in each day in the dataset DS.

Data Availability

The data used in this study are available from the corresponding author upon reasonable request.

Conflicts of Interest

The authors declare that they have no conflicts of interest.

References

- [1] Y. Shakrina, "A stackelberg game inspired model of real-time economic dispatch with demand response," M.Sc. Thesis, Lebanese American University, Beirut, Lebanon, 2021.
- [2] R. Deng, Z. Yang, M. Y. Chow, J. Chen, M. Chow, and J. Chen, "A survey on demand response in smart grids: mathematical models and approaches," *IEEE Transactions on Industrial Informatics*, vol. 11, no. 3, pp. 570–582, 2015.
- [3] A. Safdarian, M. Fotuhi-Firuzabad, M. Lehtonen, and M. Lehtonen, "Benefits of demand response on operation of distribution networks: a case study," *IEEE Systems Journal*, vol. 10, no. 1, pp. 189–197, 2016.
- [4] K. Kopsidas, M. Abogaleela, and M. Abogaleela, "Utilizing demand response to improve network reliability and ageing resilience," *IEEE Transactions on Power Systems*, vol. 34, no. 3, pp. 2216–2227, 2019.
- [5] K. Kopsidas, A. Kapetanaki, V. Levi, and V. Levi, "Optimal demand response scheduling with real-time thermal ratings of overhead lines for improved network reliability," *IEEE Transactions on Smart Grid*, vol. 8, no. 6, pp. 2813–2825, 2017.
- [6] E. Parizy, H. R. Bahrami, S. Choi, H. R. Bahrami, and S. Choi, "A low complexity and secure demand response technique for peak load reduction," *IEEE Transactions on Smart Grid*, vol. 10, no. 3, pp. 3259–3268, 2019.
- [7] N. Ul Hassan, Y. I. Khalid, C. Yuen, W. I. Tushar, C. Yuen, and W. Tushar, "Customer engagement plans for peak load reduction in residential smart grids," *IEEE Transactions on Smart Grid*, vol. 6, pp. 3029–3041, 2015.
- [8] S. Madaeni, R. H. Sioshansi, and R. Sioshansi, "Using demand response to improve the emission benefits of wind," *IEEE Transactions on Power Systems*, vol. 28, no. 2, pp. 1385–1394, 2013.
- [9] A. R. Jordehi, "Optimisation of demand response in electric power systems, a review," *Renewable and Sustainable Energy Reviews*, vol. 103, pp. 308–319, 2019.
- [10] H. Roh, J. W. Lee, and J. Lee, "Residential demand response scheduling with multiclass appliances in the smart grid," *IEEE Transactions on Smart Grid*, vol. 7, no. 1, pp. 94–104, 2016.
- [11] M. Javadi, A. E. Nezhad, P. H. Nardelli et al., "Self-scheduling model for home energy management systems considering the end-users discomfort index within price-based demand response programs," *Sustainable Cities and Society*, vol. 68, Article ID 102792, 2021.
- [12] J. Zhu, Y. Lin, W. Lei et al., "Optimal household appliances scheduling of multiple smart homes using an improved cooperative algorithm," *Energy*, vol. 171, pp. 944–955, 2019.
- [13] R. Morsali, G. S. Thirunavukkarasu, M. Seyedmahmoudian et al., "A relaxed constrained decentralised demand side management system of a community-based residential microgrid with realistic appliance models," *Applied Energy*, vol. 277, Article ID 115626, 2020.
- [14] J. Yao, G. T. Costanzo, G. Zhu, B. T. Wen, G. Zhu, and B. Wen, "Power admission control with predictive thermal management in smart buildings," *IEEE Transactions on Industrial Electronics*, vol. 62, no. 4, pp. 2642–2650, 2015.
- [15] H. Wang, Y. Zheng, M. Zhou, and M. Zhou, "Unit scheduling considering the flexibility of intelligent temperature control appliances under TOU power price," *International Journal of Electrical Power & Energy Systems*, vol. 125, Article ID 106477, 2021.
- [16] M. Alcázar-Ortega, C. Álvarez-Bel, G. Escrivá-Escrivá, A. Domijan, G. Escrivá-Escrivá, and A. Domijan, "Evaluation and assessment of demand response potential applied to the meat industry," *Applied Energy*, vol. 92, pp. 84–91, 2012.
- [17] D. Olsen, S. Goli, D. Faulkner, and A. McKane, "Opportunities for energy efficiency and DR in the California cement industry," *Ernest Orlando Lawrence Berkeley Nat. Lab., PIER Industrial/Agricultural/Water End-Use Energy Efficiency Program*, LBL Publications, Madhya Pradesh, India, 2010.
- [18] M. Alcazar-Ortega, "Evaluation and assessment of new demand response products based on the use of flexibility in industrial processes: application to the food industry," Thesis, University Of South Florida, Tampa, FL, USA, 2011.
- [19] Y. Li, S. H. Hong, and S. H. Hong, "Real-time demand bidding for energy management in discrete manufacturing facilities," *IEEE Transactions on Industrial Electronics*, vol. 64, no. 1, pp. 739–749, 2017.
- [20] N. Gerami, A. Ghasemi, A. Lotfi et al., "Energy consumption modeling of production process for industrial factories in a day ahead scheduling with demand response," *Sustainable Energy, Grids and Networks*, vol. 25, Article ID 100420, 2021.
- [21] R. Lu, R. Bai, Y. Huang et al., "Data-driven real-time price-based demand response for industrial facilities energy management," *Applied Energy*, vol. 283, Article ID 116291, 2021.
- [22] X. Zhang, G. Hug, J. Z. Kolter, I. Harjunkoski, J. Z. Kolter, and I. Harjunkoski, "Demand response of ancillary service from industrial loads coordinated with energy storage," *IEEE Transactions on Power Systems*, vol. 33, no. 1, pp. 951–961, 2018.
- [23] Y. Shakrina, H. Margossian, and H. Margossian, "A Stackelberg game-inspired model of real-time economic dispatch

- with demand response,” *International Transactions on Electrical Energy Systems*, vol. 31, no. 11, Article ID e13076, 2021.
- [24] R. Wang, D. Ma, M. J. Li et al., “Accurate current sharing and voltage regulation in hybrid wind/solar systems: an adaptive dynamic programming approach,” *IEEE Transactions on Consumer Electronics*, vol. 68, no. 3, pp. 261–272, 2022.
- [25] R. Wang, Q. Sun, W. Hu et al., “SoC-based droop coefficients stability region analysis of the battery for stand-alone supply systems with constant power loads,” *IEEE Transactions on Power Electronics*, vol. 36, no. 7, pp. 7866–7879, 2021.
- [26] Z. Tang, Y. Liu, J. Liu et al., “Multi-stage sizing approach for development of utility-scale BESS considering dynamic growth of distributed photovoltaic connection,” *Journal of Modern Power Systems and Clean Energy*, vol. 4, no. 4, pp. 554–565, 2016.
- [27] X. Lu, K. Zhou, C. Zhang, S. Yang, C. Zhang, and S. Yang, “Optimal Load Dispatch for industrial manufacturing process based on demand response in a smart grid,” *Journal of Renewable and Sustainable Energy*, vol. 10, no. 3, Article ID 35503, 2018.
- [28] T. Weitzel, C. H. Glock, and C. H. Glock, “Scheduling a storage-augmented discrete production facility under incentive-based demand response,” *International Journal of Production Research*, vol. 57, no. 1, pp. 250–270, 2019.
- [29] C. Huang, H. Zhang, Y. Song et al., “Demand response for industrial micro-grid considering photovoltaic power uncertainty and battery operational cost,” *IEEE Transactions on Smart Grid*, vol. 12, no. 4, pp. 3043–3055, 2021.
- [30] G. Xu, C. Shang, S. Fan et al., “Sizing battery energy storage systems for industrial customers with photovoltaic power,” *Energy Procedia*, vol. 158, pp. 4953–4958, 2019.
- [31] E. M. Urbano, V. Martinez-Viol, K. Kampouropoulos, and L. Romeral, “Renewable energy source and storage systems sizing optimization for industrial prosumers,” in *Proceedings of the 2020 25th IEEE International Conference on Emerging Technologies and Factory Automation (ETFA) 1741-1748*, Vienna, Austria, September 2020.
- [32] G. Carpinelli, A. Fazio, S. Khormali, F. R. Mottola, S. Khormali, and F. Mottola, “Optimal sizing of battery storage systems for industrial applications when uncertainties exist,” *Energies*, vol. 7, no. 1, pp. 130–149, 2014.
- [33] M. Islam, Z. M. Sun, and Z. Sun, “Onsite generation system sizing for manufacturing plant considering renewable sources towards sustainability,” *Sustainable Energy Technologies and Assessments*, vol. 32, pp. 1–18, 2019.
- [34] G. Mohy-ud-din, D. H. Vu, K. M. Muttaqi, D. Sutanto, and D. Sutanto, “An integrated energy management approach for the economic operation of industrial microgrids under uncertainty of renewable energy,” *IEEE Transactions on Industry Applications*, vol. 56, no. 2, pp. 1062–1073, 2020.
- [35] J. Lee, “Mixed-integer nonlinear programming: some modeling and solution issues,” *IBM Journal of Research and Development*, vol. 51, no. 3.4, pp. 489–497, 2007.
- [36] J. B. MacQueen, *Some Methods for Classification and Analysis of Multivariate Observations*, Defense Technical Information Center, Fort Belvoir, VI, USA, 1966.
- [37] S. Lloyd, “Least squares quantization in PCM,” *IEEE Transactions on Information Theory*, vol. 28, no. 2, pp. 129–137, 1982.
- [38] M. Kaut, “Scenario generation by selection from historical data,” *Computational Management Science*, vol. 18, no. 3, pp. 411–429, 2021.
- [39] Nordpool, “Historical market data,” <https://www.nordpoolgroup.com/historical-market-data/>.